Available online at www.sciencedirect.com
ScienceDirect
Mendeleev Commun., 2010, **20**, 161–164
Mendeleev Communications

Electron-density and electrostatic-potential features of orthorhombic chlorine trifluoride

Anastasia V. Shishkina,[a] Adam I. Stash[a,b] Bartolomeo Civalleri,[c] Arkady Ellern[d] and Vladimir G. Tsirelson*[a]

[a] *D. I. Mendeleev University of Chemical Technology of Russia, 125047 Moscow, Russian Federation. Fax: +7 499 978 9584; e-mail: tsirel@muctr.edu.ru*
[b] *L. Ya. Karpov Institute of Physical Chemistry, 103064 Moscow, Russian Federation. E-mail: adam@cc.nifhi.ac.ru*
[c] *Università di Torino and NIS Centre of Excellence, 10125 Torino, Italy. E-mail: bartolomeo.civalleri@unito.it*
[d] *Iowa State University, Ames, IA, 50011, USA. E-mail: Ellern@iastate.edu*

DOI: 10.1016/j.mencom.2010.05.013

The intermolecular interactions in solid ClF_3 are analyzed in terms of the quantum theory of atoms in molecules and crystals using experimental and theoretical electron density.

The ClF_3 molecules in a crystal are held together by the van der Waals forces, which manifest themselves by the appearance of the electron-density bridges linking the neighboring molecules.[1] The mechanics of intermolecular van der Waals bonding is the same as that of the closed-shell intramolecular bonding;[1(a)] however, the electron density in the intermolecular space of solid ClF_3 is very small and rather flat. It makes difficult the reconstruction of the electron density from the high-resolution X-ray diffraction data. In addition, ClF_3 is a very strong oxidizing and fluorination agent, which is extremely reactive toward most inorganic and organic materials.[1(c),(f),2] It is non-flammable in air but supports combustion with almost all organic vapours and liquids. These facts not only result in difficulties in obtaining the stable ClF_3 single crystal of good diffraction quality but also make its X-ray diffraction study nontrivial.[3] The quantum-chemical determination of tiny intermolecular electron-density bridges meets a similar problem due to the lack of a proper description of the electron correlation in the intermolecular regions.[4]

Here, we describe for the first time the electron-density features of the atomic and molecular interactions in an orthorhombic ClF_3 crystal by using the low-temperature experimental X-ray diffraction data[†,‡] and high-level theoretical[§] computation of a three-dimensional periodical crystal. We also present the electrostatic-potential features revealing the nature of the attractive electrostatic interaction, which exists between the atoms in solid ClF_3 even though they carry the same-sign formal charge. The quantum theory of atoms in molecules and crystals (QTAIMC),[5] which provides a basis for a comprehensive description of bonding in molecules and crystals, is applied for these purposes.

The network of the bond paths in electron density[5] reflecting the electron-density (ED) bridges linking both atoms in molecules and the neighboring molecules was revealed (Figures 1 and 2). In an orthorhombic ClF_3 crystal, the molecules form the layers parallel to the (100) plane. Each layer consists of ribbons along the z axis with the shortest intermolecular F(2)–F(2) contact of 2.687 Å perpendicular to the (010) plane. The shortest Cl–F(1) distance between molecules in the ribbons is 3.421 Å. The Cl–F and F–F distances between the ribbons belonging to different layers are in the range from 3.064 to 3.409 Å and from 2.966 to 3.288 Å, respectively. A molecule in a crystal has 14 neighboring molecules; each Cl atom has 8 neighboring F atoms while the F atoms have 6 adjoining atoms. Note that the atomic positional parameters derived in this work agree within one e.s.d. with those derived by the X-ray diffraction at the same temperature.[2(a)]

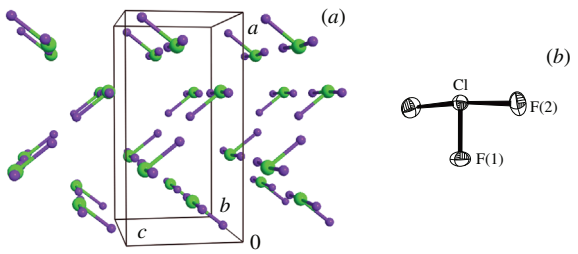

Figure 1 (*a*) Molecular structure of an orthorhombic crystal of ClF_3 and (*b*) the standard presentation of a ClF_3 molecule.

The Hirshfeld test showed that the restricted diffraction quality of our ClF_3 specimen did not allow reaching the complete separation of aspheric electron-density features and the effects

† Chlorine trifluoride was synthesized according to a published procedure.[6] Traces of HF were removed by heating the resulting mixture for 24 h in a monel autoclave over NaF pre-dried in a vacuum at 500 °C. 4-Fold trap-to-trap distillation in the monel-stainless steel vacuum system resulted in a chromatographically pure sample without traces of HF and ClF_5. Thermal analysis of the sample was in a good agreement with the published data for a melting point of pure ClF_3 of –76.3 °C.[7] A thin-walled quartz capillary (diameter of 0.4 mm) was connected to the vacuum line and ClF_3 was condensed into several times in order to passivate the glass surface. After that the capillary was pumped under heating (400 °C) for 24 h. The passivated capillary was filled with a fresh portion of ClF_3 by vacuum condensation, seeled while frozen and transferred to the X-ray diffractometer without interrupting the cooling process. The single crystal (0.4×0.4×1.0 mm, cylinder) was grown at approximately –80 °C by cooling with a gradient of 5 K h^{-1} to crystallize a low-temperature orthorhombic modification, which is stable below –83.1 °C.[3]

Crystallographic data: crystal of ClF_3 is orthorhombic at 153 K, space group *Pnma*, $a = 8.8101(9)$, $b = 6.0995(6)$ and $c = 4.5145(4)$ Å, $V = 242.60(4)$ Å^3, $Z = 4$, μ(MoKα) = 13.7 cm^{-1}. Intensities of 5646 diffraction reflections ($-14 < h < 17$, $-11 < k < 10$, $-8 < l < 8$; $\sin\theta/\lambda \leq 1.0$ Å^{-1}) were measured at 153.0(2) K with a Bruker CCD-1000 diffractometer [λ(MoKα) = 0.71073 Å, $\theta = 45.65°$]; 879 independent reflections with $I > 2\sigma(I)$ were obtained; $R_{int} = 0.071$. The unit cell parameters were obtained from three series of ω scans at different starting angles. Each series consisted of 30 frames collected at intervals of 0.3° in a 10° range about ω with an exposure time of 5 s per frame. The obtained reflections were successfully indexed by an automated indexing routine built in the SMART program.

© 2010 Mendeleev Communications. All rights reserved.

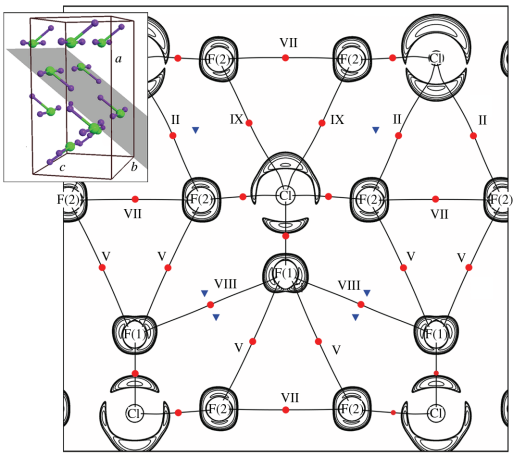

Figure 2 Distribution of the Laplacian of the model electron density was derived from the X-ray diffraction experiment. Only positive Laplacian values are shown; the line intervals are 2×10^n, 4×10^n and 8×10^n e Å^{-5} ($-2 \le n \le 2$). The critical points (3, –1) and (3, +1) in electron density are marked by circles and triangles, respectively.

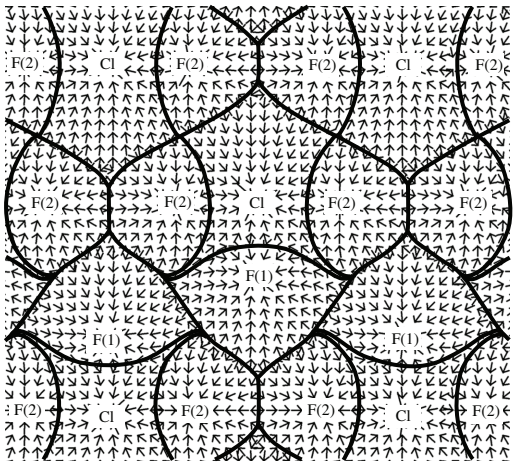

Figure 3 Experimental inner-crystal vector electric field (see Figure 2) in the unit cell of solid ClF_3. Thick lines indicate the limits of φ-basins.

of atomic displacements. Unfortunately, all our efforts to improve the data by correcting the primary measured data set and performing the new refinements by modifying the structural model have failed. We have also undertaken the attempts to perform new measurements; however, we were unable to get a crystalline ClF_3 specimen of better diffraction quality and to collect the superior experimental data. Nevertheless, the level of the random error in the experimental ED estimated *via* e.s.d. in the multipole parameters[19] proved to be 0.04 e Å^{-3} at the bond critical points of the Cl–F(1) and Cl–F(2) intramolecuar bonds, while between atoms involved in the van der Waals interactions it is only 0.002 e Å^{-3}. The ED in the middle of intermolecular distances in ClF_3 varies from 0.02 to 0.06 e Å^{-3}, well above the error bar. The experimental and theoretical ED parameters of the intra- and intermolecular bond critical points in ClF_3, reconstructed *via* the multipole model, reasonably match each other (see Table 1S in Online Supplementary Materials). The Laplacian of electron density, $\nabla^2\rho_b(\boldsymbol{r})$, is positive (closed-shell interactions) and ranges between molecules from 0.36 to 0.96 e Å^{-5}. This agrees with the QTAIMC analyses of both theoretical and experimental ED in other van der Waals molecular systems,[1(a),(c),(f)–(i)] which show the flat distribution of electron density in the inter-

The data were collected using the full sphere routine by collecting four sets of the low-angle frames with 0.3° scans in ω with an exposure time of 5 s per frame and three sets of the high-angle frames with an exposure time of 30 s per frame. After the background subtraction, the whole data set was corrected for Lorentz and polarization effects.

The structure of ClF_3 was solved by a direct method and refined by the full-matrix least-squares technique against F^2 using the spherical-atom model and the anisotropic harmonic approximation for atomic displacements ($R = 0.042$, $wR = 0.118$, GOF = 1.13). The atomic relativistic scattering factors and anomalous scattering corrections were taken from ref. 8. Isotropic secondary extinction considered according to Becker and Coppens[9] was found to be negligible. All calculations were performed using the SHELXTL (version 5.1) program library.[10]

Atomic coordinates, bond lengths, bond angles and thermal parameters have been deposited at the Inorganic Crystal Structure Database (ICSD). These data can be obtained free of charge *via* http://www.fiz-karlsruhe.de/obtaining_crystal_structure_data.html (or from the ICSD, Fachinformationszentrum Karlsruhe, 76344 Eggenstein-Leopoldshafen, Germany; fax: +49 7247 808 666; or crysdata@fiz-karlsruhe.de). Any request to the ICSD for data should quote the full literature citation and ICSD reference number 421387.

‡ The Hansen and Coppens[11(a)] multipole structural model at the hexadecupole level (program MOLDOS97/MOLLY[11]) was employed in a refinement based on $|F|$ with weights $w = 0.5/[\sigma^2(|F|) + 0.0001F^2]$; 759 independent reflections with $I > 3\sigma(I)$ were used: $R = 0.024$, $wR = 0.034$, GOF = 1.20. Both core and valence electron shells were described by the atomic many-configuration relativistic wave functions.[12,13] Anomalous dispersion corrections were taken into account.[8] The atomic displacements were described in the anharmonic approximation using the Gram–Charlier expansion of temperature factor up to the tensors of fourth rank.[13] The significance of the structural model of ClF_3 was checked using the Hamilton[14(a)] test, which showed that the account of anharmonicity is significant at a 0.05 level. The validity of the refinement was also controlled by the Abrahams–Keve[14(b)] plot and the Hirshfeld rigid bond test[14(c)] (Δ[Cl(1)–F(1)] = 0.0022 Å^2; Δ[Cl(1)–F(2)] = 0.0046 Å^2). All the experimental-density-based calculations were done with the WinXPRO program.[15] The maps of experimental deformation electron density and residual density are placed to Online Supplementary Materials.

§ Calculations on the ClF_3 crystal have been carried out within the Kohn–Sham formalism at the B3LYP-D* level corresponding to the B3LYP functional augmented with a damped empirical pair-wise correction term (*i.e.*, $-f_{dmp}C_6/R^6$) to include long-range dispersion interactions.[16] A development version of the CRYSTAL06 code[17(a),(b)] has been used. The accuracy level was controlled by five values that were set to 7 7 7 7 14. The (75,975)p atomic grid has been used with 75 radial points within the Gauss–Legendre and 975 angular points on the Lebedev surface in the most accurate integration region. The shrinking factor of the commensurate reciprocal-space grid was set to 4, corresponding to 27 independent $\boldsymbol{k}$-vectors in the irreducible Brillouin zone. It was found that tighter parameters affected computed results only marginally; therefore, the accuracy in one- and two-electron integrals calculation, DFT numerical integration and sampling of the reciprocal space were adequate to model the crystalline structure of ClF_3.

A full crystal geometry optimization[17(c)] was carried out using analytical energy gradients.[17(d),(e)] Convergence was tested on the rms and the absolute value of the largest component of the gradients and the estimated displacements. The crystal structure optimization was considered complete when the maximum force, the rms force, the maximum atomic displacement and the rms atomic displacement were simultaneously satisfied to values of 0.00045, 0.00030, 0.00180 and 0.00120 a.u., respectively. Vibration frequencies at the Γ point[17(f)] were computed through the numerical differentiation of analytical energy gradients.

Nine different TZ and QZV basis sets from Ahlrichs' family with increasing number of atomic functions were employed ranging from 438 to 800 functions in the unit cell. Details on the basis set choice and discussion of calculations will be published elsewhere.[18] We found that a QZV2P basis set is the minimal choice that leads to the correct crystalline *Pnma* phase. It did not show any imaginary frequency and yielded good agreement with X-ray measurements ($a = 8.720$, $b = 6.239$ and $c = 4.525$ Å). Then, the multipole refinement was carried out within the Hansen–Coppens formalism[11(a)] using the structure factors obtained from the QZV2P wave function [1818 independent reflections with $I > 3\sigma(I)$, $\sin\theta/\lambda \le 1.0$ Å^{-1}; $R = 0.004$, $wR = 0.004$, GOF = 1.11]. It allowed us to compare the electron-density features derived in the same manner.

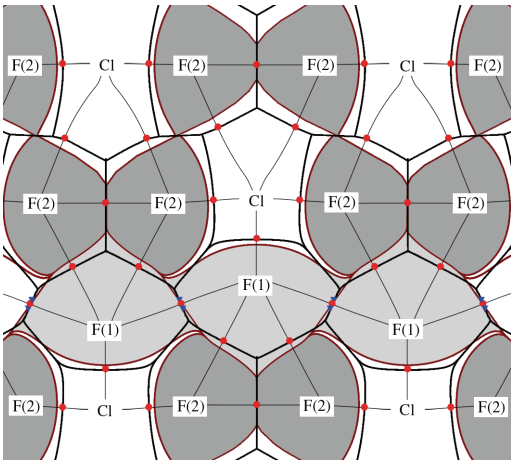

Figure 4 Superposition of interatomic surfaces of ρ-basins and φ-basins (experiment). The bond paths are shown by the thin lines. The interatomic surface of ρ-basins is marked by thick lines, φ-basins of Cl, F(1) and F(2) atoms are depicted over white, bright grey and dark grey, respectively. The critical points (3, –1) in electron density are shown by small circles.

molecular regions with $\rho_b(\boldsymbol{r}) \sim 0.02$–$0.07$ e Å^{-3} and $\nabla^2\rho_b(\boldsymbol{r}) \sim$ $\sim +(0.20$–$0.85)$ e Å^{-5}. The atomic basins in the electron density (ρ-basins) limited by the surfaces S defined by the condition $\nabla\rho(\boldsymbol{r})\cdot\boldsymbol{n}(\boldsymbol{r}) = 0$, where $\boldsymbol{n}(\boldsymbol{r})$ is a unit vector normal to the surface S at $\boldsymbol{r}$, showed the aspheric shapes (Figure 4) and comparable sizes. The experimental atomic volumes are 17.508, 15.130 and 13.982 Å^3 for Cl, F(1) and F(2), respectively. As these volumes are proportional to the atomic polarizabilities and reflect the additive contributions to the molecular polarizability,[20(a)] it can be supposed that all the atoms yield comparable contributions to the dispersion interaction of molecules in crystalline ClF_3. The atomic electron populations computed by the integration of experimental and theoretical ED within the atomic ρ-basins allowed us to determine the atomic charges, which are given in Table 2S. They show that the atom F(2) carries a higher negative net charge.

The dipole–dipole molecular interactions define the general packing motif in the crystalline ClF_3, while the tiny packing details can be described in terms of molecular recognition.[1(i),20] The latter is due to the intermolecular van der Waals interactions and may be interpreted by using the concept of molecular complementarity. It shows two limiting cases: the first, a van der Waals complementarity, is determined by the size and shape of contacting atoms or atomic groups; the second, a Lewis complementarity, is responsible for the assembly of the molecules by adjustment of their electrophilic and nucleophilic (acid and base) molecular sites. Analysis of the Laplacian of the electron density, $\nabla^2\rho(\boldsymbol{r})$, allows us to distinguish these cases.[1(i),20(b),(c)]. The peaks of local concentrations in valence-shell ED, where $\nabla^2\rho(\boldsymbol{r}) < 0$, indicate the nucleophilic molecular sites, while the local areas of the valence-shell ED depletion (the holes where $\nabla^2\rho(\boldsymbol{r}) > 0$), locate the electrophilic activity sites. The Lewis complementary corresponds to fitting of lumps and holes in adjacent molecules, as observed for solid Cl_2,[1(c)] ClF,[1(f)] S_4N_4,[1(h)] N_2O_4,[1(i)] C_6Cl_6,[21(a)] As_2O_5, AsO_2 and As_2O_3.[21(b)] In contrast, a van der Waals complementarity does not exhibit the evident peak-to-hole fitting of adjacent molecules and the specificity of its mechanism has not been established yet in detail.

To establish which type of molecular complementarity dominates in orthorhombic ClF_3, the Laplacians of experimental and theoretical EDs were computed (see Figure 2 and Figures 3S, 4S, 5S in Online Supplementary Materials). The maps displaying the areas of function $\nabla^2\rho < 0$ superimposed with the bond paths in ClF_3 show that the concentrations in the valence-shell ED as appeared in the function $\nabla^2\rho(\boldsymbol{r})$ form the tori around the F atoms (see the inserts in Figure 3S), no noticeable peaks were found. In contrast, the well-localized $-\nabla^2\rho(\boldsymbol{r})$ peaks in the valence shells of Cl atoms are present and can be associated with the electron lone pairs. However, these peaks do not lead to the peak-to-hole fitting in adjacent molecules. Thus, Figure 2 and Figures 3S, 4S, 5S allow us to conclude that a van der Waals complementarity dominates in orthorhombic ClF_3.

We can speculate that the absence of evident peak-to-hole interactions can be related to the small values in the electron density bridges between ClF_3 molecules reflecting the weak bond directivity of the intermolecular F–F and F–Cl contacts in solid ClF_3.

To understand the features of the electrostatic contributions to the atom–atom interactions in ClF_3, we have considered the inner-crystal electrostatic field, $\boldsymbol{E}(\boldsymbol{r}) = -\nabla\varphi(\boldsymbol{r})$, where $\varphi(\boldsymbol{r})$ is electrostatic potential. The field $\boldsymbol{E}(\boldsymbol{r})$ defines the classic inner-crystal electrostatic force $\boldsymbol{F}(\boldsymbol{r}) = q\boldsymbol{E}(\boldsymbol{r})$ acting on the charge q at point $\boldsymbol{r}$. Nuclei of neighboring atoms in any crystal are separated in the fields $\boldsymbol{E}(\boldsymbol{r})$ and $\boldsymbol{F}(\boldsymbol{r})$ by surfaces P_i, satisfying the zero-flux condition $\boldsymbol{E}(\boldsymbol{r})\cdot\boldsymbol{n}(\boldsymbol{r}) = \boldsymbol{F}(\boldsymbol{r})\cdot\boldsymbol{n}(\boldsymbol{r}) = 0$, $\forall\boldsymbol{r} \in P_i(\boldsymbol{r})$; $\boldsymbol{n}(\boldsymbol{r})$ is a unit vector normal to the surface P_i at $\boldsymbol{r}$. Each surface P_i defines the φ-basin of ith atom, inside of which the electrons are attracted to the nuclei i.[22] The $\nabla\varphi(\boldsymbol{r})$ gradient field allows us to highlight the network of the atomic-like φ-basins in solid ClF_3 (Figure 3). It allows revealing the network of atomic electrostatic interactions in this crystal. Indeed, as the electron density within each φ-basin is attracted to the corresponding nucleus, the overlap of the ρ-basins and φ-basins of adjacent atoms A and B leads to situation in which the part of the ED belonging to the A atom falls into φ-basin of the B atom (Figure 4). In solid ClF_3, the ρ-basins of F(1) and F(2) atom overlap the φ-basins of Cl atom both within each molecule and between the neighboring molecules (Cl–F contacts numbering as I, II, III, IV and IX; see Table 1S). The same applies to the contact F(2)–F(1) (V). That provides the physical basis for electrostatic atom–atom attraction in ClF_3 crystal. It also explains why the attractive electrostatic interaction exists between the atoms in solid ClF_3 even though they carry the same-sign formal net charge.

Note that the formation of the intermolecular bond paths in electron density is not always accompanied by the overlap of the atomic ρ-basins and φ-basins. For example, the boundaries of the ρ-basin and φ-basin of F(2)–F(2) atoms lined by the bond path (contact VII) exactly coincide (Figure 4). In general, the electrostatic-interaction picture does not exhibit the directional character and does not link with the bond paths in the electron density, which are related to quantum effects.

Thus, this work allowed us to clarify the complete picture of the intermolecular interactions in orthorhombic ClF_3. It was found that a van der Waals complementarity dominates in solid ClF_3; it is determined by the size and shape of contacting atoms and does not show the adjustment of neighboring molecules by means of fitting localized valence-shell charge concentrations and depletions. Partial overlap of atomic-like basins created by zero-flux surfaces in both the electron density and the electrostatic potential is an origin of the attractive electrostatic interaction between atoms in solid ClF_3 even though they carry the same-sign formal charge.

This work was supported by the Russian Foundation for Basic Research (grant no. 07-03-00702).

Online Supplementary Materials

Supplementary data associated with this article can be found in the online version at doi:10.1016/j.mencom.2010.05.013.

References

1 (*a*) R. G. A. Bone and R. F. W. Bader, *J. Phys. Chem*., 1996, **B100**, 10892; (*b*) R. F. W. Bader, *J. Phys. Chem*., 1998, **A102**, 7314; (*c*) V. G. Tsirelson, P. F. Zou, T. H. Tang and R. F. W. Bader, *Acta Crystallogr*., 1995, **A51**, 143; (*d*) J. Hernańdez-Trujillo and R. F. W. Bader, *J. Phys. Chem*., 2000, **A104**, 1779; (*e*) R. F. W. Bader, J. Hernańdez-Trujillo and F. Corteś-Guzmań, *J. Comput. Chem.*, 2007, **28**, 4; (*f*) R. Boese, A. D. Boese, D. Blaser, M. Yu. Antipin, A. Ellern and K. Seppelt, *Angew. Chem., Int. Ed. Engl*., 1997, **36**, 1489; (*g*) R. Boese, D. Blaser, O. Heinemann, Yu. Abramov, V. G. Tsirelson, P. Blaha and K. Schwarz, *J. Phys. Chem*., 1999, **A103**, 6209; (*h*) W. Scherer, M. Spiegler, B. Pedersen, M. Tafipolsky, W. Hieringer, B. Reinhard, A. J. Downs and G. S. McGrady, *Chem. Commun*., 2000, 635; (*i*) V. G. Tsirelson, A. V. Shishkina, A. I. Stash and S. Parsons, *Acta Crystallogr.*, 2009, **B65**, 647.

2 (*a*) R. D. Burbank and F. N. Bensey, *J. Chem. Phys*., 1953, **21**, 602; (*b*) A. J. Edwards and R. J. C. Sills, *J. Chem. Soc. A*, 1970, 2697; (*c*) G. Skirrow and H. G. Wolfhard, *Proc. R. Soc. London*, 1955, **A232**, 78.

3 M. Yu. Antipin, A. M. Ellern, V. F. Sukhoverkhov and Yu. T. Struchkov, *Zh. Neorg. Khim*., 1989, **34**, 823 (*Russ. J. Inorg. Chem*., 1989, **34**, 459).

4 Y. Zhao and D. G. Truhlar, *Acc. Chem. Res*., 2008, **41**, 157.

5 R. F. W. Bader, *Atoms in Molecules: A Quantum Theory*, Clarendon Press, Oxford, 1990.

6 V. G. Tsirelson, *Quantum Chemistry. Molecules, Molecular Systems and Solids*, Binom Publ., Moscow, 2010.

7 O. Ruff and H. Krug, *Z. Anorg. Allg. Chem*., 1930, **190**, 270.

8 *International Tables for Crystallography*, ed. A. J. C. Wilson, Kluwer Academic Publishers, Dordrecht, 1995, vol. C.

9 P. J. Becker and P. Coppens, *Acta Crystallogr*., 1974, **A30**, 129.

10 (*a*) G. M. Sheldrick, *Acta Crystallogr*., 2008, **A64**, 112; (*b*) G. M. Sheldrick, *Bruker Analytical X-Ray Systems*, Madison, WI, 2004.

11 (*a*) N. K. Hansen and P. Coppens, *Acta Crystallogr*., 1978, **A34**, 909; (*b*) J. Protas, *MOLDOS97/ MOLLY IBM PC-DOS*, 1997.

12 P. Macchi and P. Coppens, *Acta Crystsallogr.*, 2001, **A57**, 656.

13 Z. Su and P. Coppens, *Acta Crystallogr.*, 1998, **A54**, 646.

14 (*a*) W. C. Hamilton, *Acta Crystallogr*., 1965, **18**, 502; (*b*) S. C. Abrahams and E. T. Keve, *Acta Crystallogr*., 1971, **A27**, 157; (*c*) F. L. Hirshfeld, *Acta Crystallogr*., 1976, **A32**, 239.

15 (*a*) A. I. Stash and V. G. Tsirelson, *J. Appl. Crystallogr.*, 2002, **35**, 371; (*b*) A. I. Stash and V. G. Tsirelson, *Crystallogr. Rep*., 2005, **50**, 202.

16 S. Grimme, *J. Comput. Chem.*, 2006, **27**, 1787.

17 (*a*) R. Dovesi, V. R. Saunders, C. Roetti, R. Orlando, C. M. Zicovich-Wilson, F. Pascale, B. Civalleri, K. Doll, N. M. Harrison, I. J. Bush, P. D'Arco and M. Llunell, *CRYSTAL06 User's Manual*, Università di Torino, Torino, 2006; (*b*) B. Civalleri, C. M. Zicovich-Wilson, L. Valenzano and P. Ugliengo, *CrystEngComm*, 2008, **10**, 405; (*c*) B. Civalleri, P. D'Arco, R. Orlando, V. R. Saunders and R. Dovesi, *Chem. Phys. Lett*., 2001, **348**, 131; (*d*) K. Doll, V. R. Saunders and N. M. Harrison, *Int. J. Quantum Chem*., 2001, **82**, 1; (*e*) K. Doll, R. Dovesi and R. Orlando, *Theor. Chem. Acc*., 2004, **112**, 394; (*f*) F. Pascale, C. M. Zicovich-Wilson, F. L. Gejo, B. Civalleri, R. Orlando and R. Dovesi, *J. Comput. Chem*., 2004, **25**, 888.

18 B. Civalleri, A. V. Shishkina, A. I. Stash and V. G. Tsirelson, *J. Mol. Struct. (THEOCHEM)*, 2010, in press.

19 V. G. Tsirelson and R. P. Ozerov, *Electron Density and Bonding in Crystals*, Institute of Physics Publishing, Bristol, Philadelphia, 1996.

20 (*a*) R. F. W. Bader, T. A. Keith, K. M. Gough and K. E. Laidig, *Mol. Phys*., 1992, **75**, 1167; (*b*) C. F. Matta and R. F. W. Bader, *Proteins*, 2003, **52**, 360; (*c*) R. F. W. Bader, P. J. MacDougall and C. D. H. Lau, *J. Am. Chem. Soc.*, 1984, **106**, 1594.

21 (*a*) T. T. T. Bui, S. Dahaoui, C. Lecomte, G. R. Desiraju and E. Espinosa, *Angew. Chem. Int. Ed*., 2009, **48**, 3838; (*b*) G. V. Gibbs, A. F. Wallace, D. F. Cox, P. M. Dove, R. T. Downs, N. L. Ross and K. M. Rosso, *J. Phys. Chem*., 2009, **A113**, 736.

22 V. G. Tsirelson, A. S. Avilov, G. G. Lepeshov, A. K. Kulygin, J. Stahn, U. Pietsch and J. C. H. Spence, *J. Phys. Chem*., 2001, **B105**, 5068.

Received: 17th November 2009; Com. 09/3421